Available online at www.sciencedirect.com
SCIENCE DIRECT®
International Journal of Heat and Mass Transfer 47 (2004) 5303–5312
International Journal of HEAT and MASS TRANSFER
www.elsevier.com/locate/ijhmt

The extended Graetz problem with piecewise constant wall temperature for pipe and channel flows

B. Weigand *, D. Lauffer

Institute of Aerospace Thermodynamics, Stuttgart University, Pfaffenwaldring 31, 70569 Stuttgart, Germany

Received 19 January 2004; received in revised form 28 May 2004
Available online 24 August 2004

Abstract

Axial heat conduction effects within the fluid can be important for duct flows if the Prandtl number is relatively low (liquid metals). In addition, axial heat conduction effects within the flow might also be important, if the heating zone is relatively short in length. The present paper shows an entirely analytical solution to the extended Graetz problem with piecewise constant wall temperature boundary conditions. The solution is based on a selfadjoint formalism resulting from a decomposition of the convective diffusion equation into a pair of first order partial differential equations. The obtained analytical solution is as simple to compute as the one without axial heat conduction. The analytical results are compared to available numerical calculations and good agreement is found.

1. Introduction

The prediction of the heat transfer characteristics in pipe and channel flows is of theoretical interest and practical importance. Heat transfer for hydrodynamically fully-developed pipe and channel flows has therefore attracted a lot of researchers in the past. Normally, the effect of streamwise conduction in the flow on the heat transfer can be neglected. The classical Graetz problem deals with heat transfer in the thermal developing region of the flow under such conditions. Good reviews on this subject for laminar and turbulent flows can be found in [1,2].

However, if the Peclet number ($Pe_D = Re_D Pr$) in the flow is small, axial heat conduction in the fluid becomes important. This is the case, for example, in compact heat exchangers where liquid metals are used as the working fluids. In addition, axial heat conduction effects in the flow might also be important for larger values of the Peclet number, if the length of the heating zone is very short. In the past, many investigations have been carried out which dealt with the solution of the extended Graetz problem (the Graetz problem considering axial heat conduction in the fluid) for thermally developing laminar flow in a pipe or in a parallel plate channel. Extensive literature reviews on this subject are given in [1,3]. Many of the solutions cited in [1,3] for the extended Graetz problem are based on the fundamental assumption that the solution of the problem has the same form of the series solution as the Graetz problem without axial heat conduction in the fluid. This approach results in a non-selfadjoint eigenvalue problem with eigenvalues that could, at least in principle, be complex and eigenvectors that could be incomplete. Several strategies have been developed in the past to overcome this problem.

* Corresponding author. Tel.: +49 711 685 3590; fax: +49 711 685 2317.
E-mail address: bw@itlr.uni-stuttgart.de (B. Weigand).

0017-9310/$ - see front matter © 2004 Elsevier Ltd. All rights reserved.
doi:10.1016/j.ijheatmasstransfer.2004.06.027

Nomenclature

a	thermal diffusivity [m^2/s]
a_1, a_2	functions
A_j	constants
c_p	specific heat at constant pressure [J/(kg K)]
D	hydraulic diameter, $4h$ (planar channel), $2R$ (circular pipe) [m]
$\vec{f}$, $\vec{S}$	vectors
F	flow index, 0 for a planar channel, 1 for a circular pipe
ΔE	relative error, $(Nu_{\text{elliptic}} - Nu_{\text{parabolic}})/Nu_{\text{elliptic}}$
h	distance between the centreline and the wall (planar duct) [m]
k	thermal conductivity [W/(mK)]
L	characteristic length, $L = h$ (planar duct), $L = R$ (circular pipe) [m]
L	matrix operator
$\tilde{n}$	coordinate [m]
$\tilde{n}$	dimensionless coordinate
Nu_D	Nusselt number based on the hydraulic diameter
p	pressure [Pa]
Pr	Prandtl number
Pe_L	Peclet number based on the characteristic length L
Pe_D	Peclet number based on the hydraulic diameter
Pr_t	turbulent Prandtl number
r	radial coordinate [m]
R	pipe radius [m]
Re_L	Reynolds number based on the characteristic length L
Re_D	Reynolds number based on the hydraulic diameter
T	temperature [K]
T_0	uniform temperature for $x \to -\infty$ [K]
T_b	bulk-temperature [K]
T_w	wall temperature [K]
u	axial velocity [m/s]
$\bar{u}_o$	axial mean velocity [m/s]
x	axial coordinate [m]
x_1	length of the heated zone [m]
$\tilde{x}$	dimensionless axial coordinate
$\hat{x}$	axial coordinate scaled by the length of the heating zone

Greek symbols

ε_{hx}	eddy diffusivity in axial direction [m^2/s]
ε_{hn}	eddy diffusivity in normal direction [m^2/s]
ε_m	eddy kinematic viscosity [m^2/s]
ρ	density [kg/m^3]
λ_j	eigenvalue
θ	dimensionless temperature
θ_b	dimensionless bulk temperature
ν	kinematic viscosity [m^2/s]
Σ	axial energy flow
$\vec{\Phi}_j$	eigenfunction

Hsu [4], for example, constructed the solution of the problem from two independent series solutions for $x < 0$ and $x > 0$. Both the temperature distribution and the temperature gradient were then matched at $x = 0$ by constructing a pair of orthonormal functions from the non-orthogonal eigenfunctions by using the Gram–Schmidt-orthonormalization procedure. Hence this method is clearly plagued with the uncertainties arising from an expansion in terms of eigenfunctions and eigenvalues belonging to a non-selfadjoint operator. However, Papoutsakis et al. [5] showed that it is possible to produce an entirely analytical solution to the extended Graetz problem for Dirichlet boundary conditions. Their solution is based on a selfadjoint formalism resulting from a decomposition of the convective diffusion equation into a pair of first order partial differential equations.

In addition several investigations have been carried out in the past concerning the extended Graetz problem in a parallel plate channel. Deavours [6] presented an analytical solution for the extended Graetz problem by decomposing the eigenvalue problem for the parallel plate channel into a system of ordinary differential equations for which he proved the orthogonality of the eigenfunctions. There are also several numerical investigations which deal with the extended Graetz problem for laminar flow in a pipe or a parallel plate channel, for example [7,8]. Hennecke [7] was one of the few, who also investigated the behaviour of the Nusselt number near the end of the heating zone. For more detailed information concerning numerical investigations the reader is referred to [1–3].

Although axial heat conduction can be ignored for turbulent convection in ordinary fluids and gases, with liquid metals this might not always be justified. In fact because of the very low Prandtl numbers for liquid metals ($0.001 < Pr < 0.06$) the Peclet number can be smaller than ten in turbulent duct flows. Lee [9] studied the extended Graetz problem in turbulent pipe flow. He found that for Peclet numbers below 100, axial heat conduction in the fluid becomes important in the thermal entrance region. He investigated a pipe which was insulated for $x < 0$ and had a uniform wall temperature for $x > 0$. Lee used the method of Hsu [4] to obtain a

series solution for the problem. Weigand [10] extended the method of Papoutsakis et al. [5] to solve the extended Graetz problem for turbulent flow inside a pipe and a parallel plate channel. This has been done by developing a new inner product between two vectors. Comparisons of the analytical solution with measurement data and numerical computations showed good agreement. Weigand et al. [11] investigated numerically the extended Graetz problem in a parallel plate channel with piecewise constant wall temperature boundary conditions. They used different turbulence models for calculating the turbulent heat flux. Their investigation showed that the normally used assumption that the eddy diffusivity in axial and normal direction are the same is correct for the range of parameters under investigation.

The purpose of the present paper is to investigate analytically the extended Graetz problem for laminar and turbulent flow in a pipe and a parallel plate channel with piecewise constant wall temperature boundary conditions. The effect of a changing length of the heating zone on the Nusselt number distribution for this boundary condition will be investigated in detail. For the case of a piecewise constant wall heat flux a similar investigation has been performed by Weigand et al. [12]. To the best knowledge of the authors, no analytical investigation is known in literature for laminar as well as for turbulent flow in pipe and channel flows for piecewise constant wall temperature conditions, which takes the axial heat conduction effect in the flow into account.

2. Analysis

Fig. 1 shows the geometrical configuration and the coordinate system. The characteristic length L denotes half of the channel height h for the flow in a parallel plate channel or the radius R for the flow in a circular pipe. It is assumed that the flow enters the duct with a hydrodynamically fully-developed laminar or turbulent velocity profile and with a uniform temperature profile

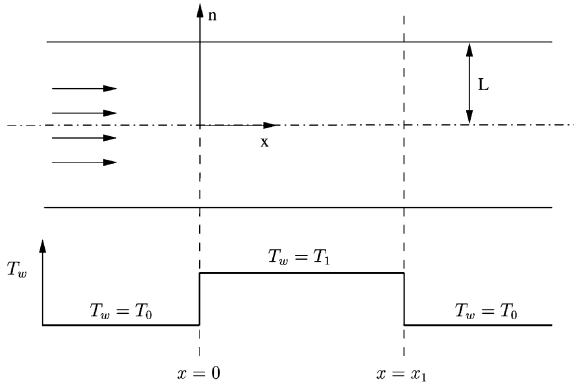

Fig. 1. Geometrical configuration and coordinate system.

T_0 for $x \to -\infty$. The wall temperature is maintained at T_0 for $x \leqslant 0$ and for $x \geqslant x_1$ and at T_1 for $0 < x < x_1$. Under the assumptions of an incompressible flow with constant physical properties, negligible viscous and turbulent energy dissipation and hydrodynamically fully-developed flow, the energy equation is given by

$$\rho c_p u(n)\frac{\partial T}{\partial x} = \frac{1}{r^F}\frac{\partial}{\partial n}\left[r^F(k+\rho c_p \varepsilon_{hn})\frac{\partial T}{\partial n}\right] + \frac{\partial}{\partial x}\left[(k+\rho c_p \varepsilon_{hx})\frac{\partial T}{\partial x}\right] \tag{1}$$

with the boundary conditions

$$\begin{aligned} &n = L: \quad T = T_0,\ x \leqslant 0 \text{ and } x \geqslant x_1,\ T = T_1,\ 0 < x < x_1 \\ &n = 0: \quad \partial T/\partial n = 0 \\ &\lim_{x\to-\infty} T = T_0 \end{aligned} \tag{2}$$

The index F which appears in Eq. (1) is equal to 0 for a planar duct and equal to 1 for a circular pipe. The velocity distribution u, which appears in Eq. (1), has been calculated from the momentum equation for hydrodynamically fully-developed flow. For a turbulent flow, the turbulent shear stress has been approximated by using a mixing length model. The reader is referred to Weigand [10] for more details. By introducing the following dimensionless quantities

$$\begin{aligned} &\theta = \frac{T-T_0}{T_1-T_0}, \quad \tilde{x} = \frac{x}{L}\frac{1}{Pe_L}, \quad \tilde{u} = \frac{u}{\bar{u}_0}, \\ &\tilde{n} = \frac{n}{L}, \quad \tilde{r} = \frac{r}{L} \\ &Pe_L = Re_L Pr, \quad Re_L = \frac{\bar{u}_0 L}{\nu}, \quad Pr = \frac{\nu}{a}, \\ &\tilde{\varepsilon}_m = \frac{\varepsilon_m}{\nu}, \quad Pr_t = \frac{\varepsilon_m}{\varepsilon_{hn}} \end{aligned} \tag{3}$$

into Eqs. (1) and (2), the energy equation can be cast into the following non-dimensional form

$$\tilde{u}\frac{\partial\theta}{\partial\tilde{x}} = \frac{1}{Pe_L^2}\frac{\partial}{\partial\tilde{x}}\left[a_1(\tilde{n})\frac{\partial\theta}{\partial\tilde{x}}\right] + \frac{1}{\tilde{r}^F}\frac{\partial}{\partial\tilde{n}}\left[\tilde{r}^F a_2(\tilde{n})\frac{\partial\theta}{\partial\tilde{n}}\right] \tag{4}$$

with the boundary conditions

$$\begin{aligned} &\tilde{n} = 1: \quad \theta = 0,\ \tilde{x} \leqslant 0 \text{ and } \tilde{x} \geqslant \tilde{x}_1,\ \theta = 1,\ 0 < \tilde{x} < \tilde{x}_1 \\ &\tilde{n} = 0: \quad \partial\theta/\partial\tilde{n} = 0 \\ &\lim_{\tilde{x}\to-\infty} \theta = 0 \end{aligned} \tag{5}$$

The functions $a_1(\tilde{n})$ and $a_2(\tilde{n})$ are given by

$$a_1(\tilde{n}) = 1 + \frac{Pr}{Pr_t}\tilde{\varepsilon}_m\left(\frac{\varepsilon_{hx}}{\varepsilon_{hn}}\right) \tag{6}$$

$$a_2(\tilde{n}) = 1 + \frac{Pr}{Pr_t}\tilde{\varepsilon}_m \tag{7}$$

In the following solution process for Eq. (4) no assumptions are required about the functions $a_1(\tilde{n})$ and $a_2(\tilde{n})$. The solution presented here holds for arbitrary functions $a_1(\tilde{n})$ and $a_2(\tilde{n})$ as long as $a_1 \geqslant 1$, $a_2 \geqslant 1$ which is obviously true from the structure of Eqs. (6) and (7). Therefore, the turbulent Prandtl number as well as the ratio $\varepsilon_{hx}/\varepsilon_{hn}$, which were used in Eqs. (6) and (7), will be specified later.

Papoutsakis et al. [5] showed that it is possible to solve Eq. (4) for laminar pipe flow ($a_1 = a_2 = 1$) by decomposing the elliptic partial differential equation into a pair of first order partial differential equations. For turbulent flows this has been shown later by Weigand [10] by using a different inner product between two vectors. The ensuing procedure for solving the here considered problem follows the method given by Refs. [5,10] for deriving the solution of the more general problem, considered here.

Let us define a function $\Sigma(\tilde{x},\tilde{n})$, which may be called the axial energy flow through a cross-sectional area of the height $\tilde{n}$ by

$$\Sigma(\tilde{x},\tilde{n}) = \int_0^{\tilde{n}} \left[\tilde{u}\theta - \frac{1}{Pe_L^2} a_1(\bar{n}) \frac{\partial\theta}{\partial\tilde{x}}\right] \tilde{r}^F \,\mathrm{d}\bar{n} \tag{8}$$

Introducing Σ, defined by Eq. (8), into the energy equation (4) results in the following system of partial differential equations

$$\frac{\partial}{\partial\tilde{x}} \vec{S}(\tilde{x},\tilde{n}) = \underset{\sim}{L}\, \vec{S}(\tilde{x},\tilde{n}) \tag{9}$$

with the two component vector $\vec{S}$ and the operator $\underset{\sim}{L}$ given by

$$\vec{S} = \begin{bmatrix} \theta(\tilde{x},\tilde{n}) \\ \Sigma(\tilde{x},\tilde{n}) \end{bmatrix}, \quad \underset{\sim}{L} = \begin{bmatrix} \dfrac{Pe_L \tilde{u}}{a_1(\tilde{n})} & -\dfrac{Pe_L^2}{\tilde{r}^F a_1(\tilde{n})} \dfrac{\partial}{\partial\tilde{n}} \\ \tilde{r}^F a_2(\tilde{n}) \dfrac{\partial}{\partial\tilde{n}} & 0 \end{bmatrix} \tag{10}$$

The boundary conditions belonging to $\Sigma(\tilde{x},\tilde{n})$ can be derived from Eqs. (5) and (8)

$$\begin{aligned} &\tilde{n} = 0: \quad \Sigma(\tilde{x},0) = 0 \\ &\lim_{\tilde{x}\to-\infty} \Sigma = 0 \end{aligned} \tag{11}$$

Before calculating the solution of Eq. (4), some interesting details about the operator $\underset{\sim}{L}$ and the corresponding eigenvalue problem for Eq. (9) should be presented. The most remarkable aspect of $\underset{\sim}{L}$ is that it gives rise to a selfadjoint problem even though the original convective diffusion operator is non-selfadjoint. This fact is of course dependent on the sort of inner product between two vectors, which will be used. If we define an inner product between two vectors

$$\vec{\Phi} = \begin{bmatrix} \Phi_1(\tilde{n}) \\ \Phi_2(\tilde{n}) \end{bmatrix}, \quad \vec{\Lambda} = \begin{bmatrix} \Lambda_1(\tilde{n}) \\ \Lambda_2(\tilde{n}) \end{bmatrix} \tag{12}$$

as

$$\left\langle \vec{\Phi}, \vec{\Lambda} \right\rangle = \int_0^1 \left[\frac{a_1(\tilde{n})\tilde{r}^F}{Pe_L^2} \Phi_1(\tilde{n})\Lambda_1(\tilde{n}) + \frac{1}{a_2(\tilde{n})\tilde{r}^F} \Phi_2(\tilde{n})\Lambda_2(\tilde{n}) \right] \mathrm{d}\tilde{n} \tag{13}$$

and the following domain for $\underset{\sim}{L}$

$$D(\underset{\sim}{L}) = \left\{ \vec{\Phi} \in H : \underset{\sim}{L}\, \vec{\Phi}(\text{exists and}) \in H, \Phi_1(1) = \Phi_2(0) = 0 \right\} \tag{14}$$

then it can be shown that $\underset{\sim}{L}$ is a symmetric operator in the Hilbert space H of interest (this means that $\langle \vec{\Phi}, \underset{\sim}{L}\, \vec{\Lambda} \rangle = \langle \underset{\sim}{L}\, \vec{\Phi}, \vec{\Lambda} \rangle$). The reader is referred for a detailed explanation to Weigand [10]. Thus the selfadjoint eigenvalue problem associated with Eq. (14) is given by

$$\underset{\sim}{L}\, \vec{\Phi}_j = \lambda_j \vec{\Phi}_j \tag{15}$$

where $\vec{\Phi}_j$ denotes the eigenvector corresponding to the eigenvalue λ_j. Using the definition of the matrix operator $\underset{\sim}{L}$ given by Eq. (10), the eigenvalue problem, Eq. (15), can be rewritten in the form

$$Pe_L^2 \left[\frac{\tilde{u}(\tilde{n})}{a_1(\tilde{n})} \Phi_{j1} - \frac{1}{\tilde{r}^F a_1(\tilde{n})} \Phi'_{j2} \right] = \lambda_j \Phi_{j1} \tag{16}$$

$$\tilde{r}^F a_2(\tilde{n}) \Phi'_{j1} = \lambda_j \Phi_{j2} \tag{17}$$

If Φ_{j2} is eliminated from Eq. (16), the following eigenvalue problem for Φ_{j1} can be obtained (see also Weigand [10])

$$\left[\tilde{r}^F a_2(\tilde{n}) \Phi'_{j1} \right]' + \tilde{r}^F \left[\frac{\lambda_j a_1(\tilde{n})}{Pe_L^2} - \tilde{u} \right] \lambda_j \Phi_{j1} = 0 \tag{18}$$

Eq. (18) has to be solved in conjunction with the boundary conditions

$$\Phi'_{j1}(0) = 0, \quad \Phi_{j1}(1) = 0 \tag{19}$$

In addition, an arbitrary normalizing condition

$$\Phi_{j1}(0) = 1 \tag{20}$$

will be used. Eq. (18) possesses both, positive eigenvalues λ_j^+ with the corresponding eigenvectors Φ_j^+ and negative eigenvalues λ_j^- with eigenvectors Φ_j^-. This is because the operator $\underset{\sim}{L}$ is neither positive nor negative definite. All λ_j are real because they are in fact the eigenvalues of a selfadjoint problem. Because the two sets of eigenvectors, normalized according to Eq. (20), constitute an orthogonal basis in H (see [5,10]) an arbitrary vector $\vec{f}$ can be expanded in terms of eigenfunctions in the following way

$$\vec{f} = \sum_{j=1}^{\infty} \frac{\langle \vec{f}, \vec{\Phi}_j \rangle}{\|\vec{\Phi}_j\|^2} \vec{\Phi}_j(\tilde{n}) \tag{21}$$

with the vector norm $\|\vec{\Phi}_j\|^2 = \langle \vec{\Phi}_j, \vec{\Phi}_j \rangle$. If we explicitly distinguish in Eq. (21) between positive and negative eigenvectors, Eq. (21) takes the following form

$$\vec{f} = \sum_{j=0}^{\infty} \frac{\langle \vec{f}, \vec{\Phi}_j^+ \rangle}{\|\vec{\Phi}_j^+\|^2} \vec{\Phi}_j^+(\tilde{n}) + \sum_{j=0}^{\infty} \frac{\langle \vec{f}, \vec{\Phi}_j^- \rangle}{\|\vec{\Phi}_j^-\|^2} \vec{\Phi}_j^-(\tilde{n}) \tag{22}$$

Now the solution of Eq. (9) can be reconsidered. The solution of the problem $\vec{S}(\tilde{x},\tilde{n})$ will be obtained in the form of the series given by Eq. (22). Therefore, the inner product appearing in the expansion coefficients of Eq. (22) must be determined. It can be shown [5,10] that

$$\langle \underset{\sim}{L}\vec{S}, \vec{\Phi}_j \rangle = \langle \vec{S}, \underset{\sim}{L}\vec{\Phi}_j \rangle + \Phi_{j2}(1) g(\tilde{x}) \tag{23}$$

The function $g(\tilde{x})$ is given by

$$g(\tilde{x}) = \begin{cases} 0, & \tilde{x} \leqslant 0,\ \tilde{x} \geqslant \tilde{x}_1 \\ 1, & 0 < \tilde{x} < \tilde{x}_1 \end{cases} \tag{24}$$

For a heating zone with half-infinite length, Eq. (24) has been given by Papoutsakis et al. [5] for laminar flow in a pipe and by Weigand [10] for turbulent flow in pipe and channel flows.

Taking the inner product of both sides of Eq. (9) with $\vec{\Phi}_j$ and using Eq. (23) one obtains

$$\frac{\partial}{\partial \tilde{x}} \langle \vec{S}, \vec{\Phi}_j \rangle = \lambda_j \langle \vec{S}, \vec{\Phi}_j \rangle + g(\tilde{x}) \Phi_{j2}(1) \tag{25}$$

Eq. (25) can be solved separately for positive and negative eigenvalues. This results in

$$\langle \vec{S}, \vec{\Phi}_j^- \rangle = C_{0j}^- \exp(\lambda_j^- \tilde{x}) + \int_{-\infty}^{\tilde{x}} (g(\tilde{x}) \Phi_{j2}^-(1)) \times \exp(\lambda_j^-(\tilde{x} - \bar{x}))\, \mathrm{d}\bar{x} \tag{26}$$

$$\langle \vec{S}, \vec{\Phi}_j^+ \rangle = C_{0j}^+ \exp(\lambda_j^+ \tilde{x}) - \int_{\tilde{x}}^{\infty} (g(\tilde{x}) \Phi_{j2}^+(1)) \times \exp(\lambda_j^+(\tilde{x} - \bar{x}))\, \mathrm{d}\bar{x} \tag{27}$$

Because the solution must be bounded for $\tilde{x} \to +\infty$ and for $\tilde{x} \to -\infty$, the two constants C_{0j}^- and C_{0j}^+, appearing in Eqs. (26) and (27) must be 0. After carrying out the integrations in Eqs. (26) and (27) the following results for $\theta(\tilde{x},\tilde{n})$, which is the first vector component of $\vec{F}(\tilde{x},\tilde{n})$, can be derived

$\tilde{x} \leqslant 0$:

$$\theta(\tilde{x},\tilde{n}) = -\sum_{j=1}^{\infty} A_j^+ \Phi_{j1}^+(\tilde{n}) \exp(\lambda_j^+ \tilde{x})[1 - \exp(-\lambda_j^+ \tilde{x}_1)] \tag{28}$$

$0 < \tilde{x} < \tilde{x}_1$:

$$\theta(\tilde{x},\tilde{n}) = \sum_{j=1}^{\infty} A_j^- \Phi_{j1}^-(\tilde{n})[\exp(\lambda_j^- \tilde{x}) - 1] - \sum_{j=1}^{\infty} A_j^+ \Phi_{j1}^+(\tilde{n}) \times [1 - \exp(\lambda_j^+(\tilde{x} - \tilde{x}_1))] \tag{29}$$

The above given equation can further be simplified by showing that $\sum_{j=1}^{\infty} \frac{\Phi_{j2}(1)\Phi_{j1}(\tilde{n})}{\lambda_j \|\vec{\Phi}_j\|^2} = 1$ (see Appendix A). Therefore, one obtains from Eq. (29)

$0 < \tilde{x} < \tilde{x}_1$:

$$\theta(\tilde{x},\tilde{n}) = 1 + \sum_{j=1}^{\infty} A_j^- \Phi_{j1}^-(\tilde{n}) \exp(\lambda_j^- \tilde{x}) + \sum_{j=1}^{\infty} A_j^+ \Phi_{j1}^+(\tilde{n}) \exp(\lambda_j^+(\tilde{x} - \tilde{x}_1)) \tag{30}$$

$\tilde{x} \geqslant \tilde{x}_1$:

$$\theta(\tilde{x},\tilde{n}) = \sum_{j=1}^{\infty} A_j^- \Phi_{j1}^-(\tilde{n}) \exp(\lambda_j^- \tilde{x})[1 - \exp(-\lambda_j^- \tilde{x}_1)] \tag{31}$$

with the constants A_j given by Refs. [5,10]

$$A_j = \frac{\Phi_{j2}(1)}{\lambda_j \|\vec{\Phi}_j\|^2} \tag{32}$$

From Eq. (30) it can be seen that the solution for $0 < \tilde{x} < \tilde{x}_1$ contains both negative and positive eigenfunctions. This shows clearly that for a heating zone of finite length axial heat conduction effects in the flow will always change the temperature field near the start and the end of the heated zone. This shows also nicely the elliptic nature of the problem under investigation.

For the designers of heat exchangers it is of great interest to know the axial variation of the Nusselt number. The Nusselt number, based on the hydraulic diameter of the duct, is defined by

$$Nu_D = \frac{D \frac{\partial T}{\partial n}\big|_{n=L}}{T_w - T_b} \tag{33}$$

where the bulk temperature T_b appearing in Eq. (33) is given by

$$T_b = \int_0^L uTr^F \,\mathrm{d}n \Big/ \int_0^L ur^F \,\mathrm{d}n \tag{34}$$

Sometimes a "modified bulk-temperature" is used instead of Eq. (34). This "mixing cup" temperature includes also the effect of axial heat conduction in the flow [15]. However, if one needs a representative mean temperature at any desired cross-section of a duct flow, probably the best information is given, according to Tamir and Taitel [15], by adopting the traditional definition given by Eq. (34).

Introducing the dimensionless quantities given by Eq. (2) into Eqs. (33) and (34) and using the temperature distribution given by Eqs. (28) and (31) results in the following expressions for the bulk-temperature

$\tilde{x} \leqslant 0$:

$$\theta_b = -(F+1) \sum_{j=1}^{\infty} A_j^+ \int_0^1 \Phi_{j1}^+(\tilde{n}) \tilde{u} \tilde{r}^F \,\mathrm{d}\tilde{n} \exp(\lambda_j^+ \tilde{x}) \times [1 - \exp(-\lambda_j^+ \tilde{x}_1)] \tag{35}$$

$0 < \tilde{x} < \tilde{x}_1$:

$$\theta_b = 1 + (F+1)\sum_{j=1}^{\infty} A_j^+ \int_0^1 \Phi_{j1}^+(\tilde{n})\tilde{u}\tilde{r}^F \,\mathrm{d}\tilde{n} \exp(\lambda_j^+(\tilde{x}-\tilde{x}_1)) + (F+1)\sum_{j=1}^{\infty} A_j^- \int_0^1 \Phi_{j1}^-(\tilde{n})\tilde{u}\tilde{r}^F \,\mathrm{d}\tilde{n} \exp(\lambda_j^-\tilde{x}) \quad (36)$$

$\tilde{x} \geqslant \tilde{x}_1$:

$$\theta_b = (F+1)\sum_{j=1}^{\infty} A_j^- \int_0^1 \Phi_{j1}^-(\tilde{n})\tilde{u}\tilde{r}^F \,\mathrm{d}\tilde{n} \exp(\lambda_j^-\tilde{x}) \times [1-\exp(-\lambda_j^-\tilde{x}_1)] \quad (37)$$

and for the Nusselt number

$\tilde{x} \leqslant 0$:

$$Nu_D = \frac{-4\sum_{j=1}^{\infty} A_j^+ \Phi_{j1}'^+(1)[\exp(\lambda_j^+\tilde{x}) - \exp(\lambda_j^+(\tilde{x}-\tilde{x}_1))]}{4^F \sum_{j=1}^{\infty} A_j^+ \int_0^1 \Phi_{j1}^+(\tilde{n})\tilde{u}\tilde{r}^F \,\mathrm{d}\tilde{n}[\exp(\lambda_j^+\tilde{x}) - \exp(\lambda_j^+(\tilde{x}-\tilde{x}_1))]} \quad (38)$$

$0 < \tilde{x} < \tilde{x}_1$:

$$Nu_D = \frac{-4\sum_{j=1}^{\infty} A_j^+ \Phi_{j1}'^+(1)\exp(\lambda_j^+(\tilde{x}-\tilde{x}_1)) - 4\sum_{j=1}^{\infty} A_j^- \Phi_{j1}'^-(1)\exp(\lambda_j^-\tilde{x})}{N} \quad (39)$$

$$N = 4^F \sum_{j=1}^{\infty} A_j^+ \int_0^1 \Phi_{j1}^+(\tilde{n})\tilde{u}\tilde{r}^F \,\mathrm{d}\tilde{n} \exp(\lambda_j^+(\tilde{x}-\tilde{x}_1)) + 4^F \sum_{j=1}^{\infty} A_j^- \int_0^1 \Phi_{j1}^-(\tilde{n})\tilde{u}\tilde{r}^F \,\mathrm{d}\tilde{n} \exp(\lambda_j^-\tilde{x}) \quad (40)$$

$\tilde{x} \geqslant \tilde{x}_1$:

$$Nu_D = \frac{-4\sum_{j=1}^{\infty} A_j^- \Phi_{j1}'^-(1)[\exp(\lambda_j^-\tilde{x}) - \exp(\lambda_j^-(\tilde{x}-\tilde{x}_1))]}{4^F \sum_{j=1}^{\infty} A_j^- \int_0^1 \Phi_{j1}^-(\tilde{n})\tilde{u}\tilde{r}^F \,\mathrm{d}\tilde{n}[\exp(\lambda_j^-\tilde{x}) - \exp(\lambda_j^-(\tilde{x}-\tilde{x}_1))]} \quad (41)$$

If the limit $\tilde{x}_1 \to \infty$ is introduced in the above given expressions for the bulk-temperature and the Nusselt number, they reduce to the expressions given by Weigand [10] for a heating zone which is half-infinite in length.

3. Results and discussion

In order to obtain solutions of the energy equation (4), the turbulent Prandtl number and the ratio ($\varepsilon_{hx}/\varepsilon_{hn}$) appearing in Eqs. (6) and (7) have to be specified. There is a variety of different models in the literature prescribing the turbulent Prandtl number. Especially in the case of liquid metal flows the values for Pr_t given by several models are quite different. A good literature review concerning different models for the turbulent Prandtl number can be found in [13]. For the results presented here the extended Kays and Crawford model of Weigand et al. [14] was used because this model was able to predict very well experimental results for the Nusselt numbers for liquid metal flows. The reader is referred to [14] for more details. The model for the turbulent Prandtl number is given by

$$Pr_t = \left(\frac{1}{2Pr_{t\infty}} + CPe_t\sqrt{\frac{1}{Pr_{t\infty}}} - (CPe_t)^2\left[1-\exp\left(-\frac{1}{CPe_t\sqrt{Pr_{t\infty}}}\right)\right]\right)^{-1} \quad (42)$$

with the quantities

$$Pe_t = \tilde{\varepsilon}_m Pr, \quad C = 0.3, \quad Pr_{t\infty} = 0.85 + \frac{100}{PrRe_D^{0.888}} \quad (43)$$

In addition the assumption was made that the ratio of the axial diffusivity to the radial diffusivity $\varepsilon_{hx}/\varepsilon_{hn}$, appearing in Eq. (6), is equal to 1. This assumption has been proven to be correct for the here considered range of parameters. The reader is referred to Weigand et al. [11] for more detailed information on this subject.

3.1. Numerical procedure and accuracy of the predictions

The eigenvalues λ_j as well as the eigenfunctions $\Phi_j(\tilde{n})$ were calculated numerically for the eigenvalue problem given by Eq. (18) by using a four-stage Runge–Kutta scheme. In order to examine the accuracy of the calculated values several calculations were carried out for laminar flows. The results for laminar pipe flow could be compared with the values given in Papoutsakis et al. [5] for different values of the Peclet number. The eigenvalues calculated here agree for the case of laminar pipe flow ($a_1 = a_2 = 1$, $\tilde{u} = 2(1-\tilde{n}^2)$) within a relative error of $|\Delta\lambda_j|/|\lambda_j| < 10^{-7}$ while the calculated constants A_j were found to be in agreement with the values given by Papoutsakis et al. [5] within a relative error of $|\Delta A_j|/|A_j| < 10^{-6}$. In addition, the calculated values for eigenvalues are in very good agreement with those of Deavours [6] for laminar flow in a parallel plate channel. For turbulent flow, the eigenvalues and constant coincide with the ones reported by Weigand [10]. Several comparisons of the analytical calculations with experimental data and numerical calculation for the special case of a heating zone which is half-infinite in length can be found in Weigand [10].

3.2. Heat transfer in a circular pipe

If the flow and heat transfer in a circular pipe is considered, the flow index F in the preceding equations must be set to 1. First we will investigate a laminar flow,

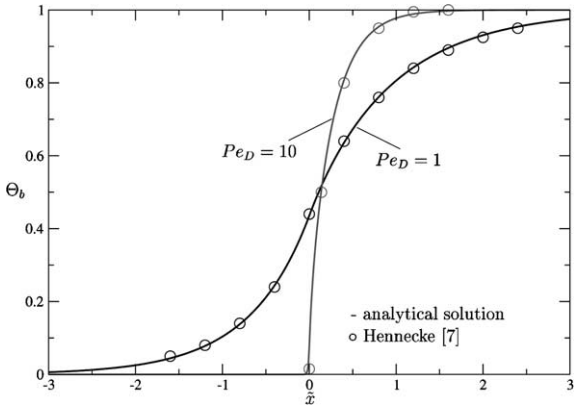

Fig. 2. Comparison between numerically [7] and analytically predicted distributions of the bulk-temperature for laminar pipe flow.

because most of the effects can be elucidated clearly for this kind of flow. For a very long heating section Hennecke [7] predicted numerically the heat transfer in a laminar pipe flow with axial heat conduction effects. Fig. 2 shows a comparison between the analytically predicted bulk-temperature and the numerical values of Hennecke. It can be seen that the agreement between both calculations is excellent for the two considered values of the Peclet number $Pe_D = 1$ and 10. Fig. 3 shows the effect of the axial heat conduction for a heating zone which is finite in length ($\tilde{x}_1 = 0.5$) for laminar flow. Fig. 3a shows the temperature distribution in the fluid near the beginning of the heating zone, whereas Fig. 3b shows the temperature profiles near the end of the heating zone. From Fig. 3a, it can clearly be seen that the temperature profile strongly deviates from the one without axial heat conduction (parabolic calculation). This is because heat is taken out from the heating zone towards the un-heated pipe section. This results in a preheating of the fluid before it approaches the heating section. Near the end of the heating section, Fig. 3b, a similar effect can be noticed. Due to the axial heat conduction effects within the flow, the fluid looses heat near the end of the heating section and the fluid temperature is lower as in the case of the parabolic situation (no axial heat conduction effects in the flow). Of course, the axial heat conduction effect influences also the distribution of the bulk-temperature. This can be seen in Fig. 4, where the distribution of the bulk-temperature is depicted for different values of the Peclet number for laminar flow. For the parabolic calculation the bulk-temperature is 0 at $\tilde{x} = 0$, because of the prescribed inlet temperature for this case. With decreasing values of the Peclet number, the bulk-temperature then obtains a flatter shape, which shows very nicely the heat transfer in axial direction. In Fig. 4, a different scaling for the x-axis has been used. The values have been plotted against $\hat{x} = \tilde{x}/\tilde{x}_1$. By

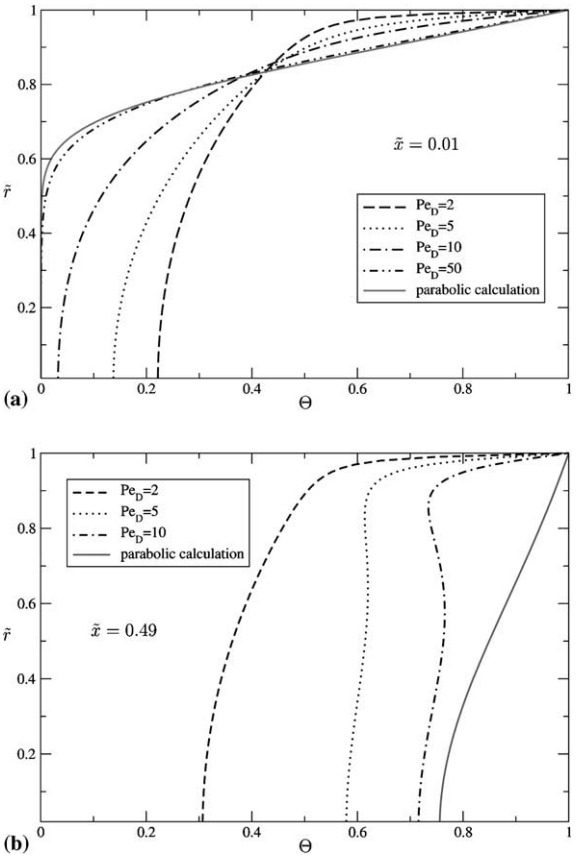

Fig. 3. Radial temperature distribution near the beginning ($\tilde{x} = 0.01$) and the end ($\tilde{x} = 0.49$) of a heating section with finite length ($\tilde{x} = 0.5$) for different values of the Peclet number (laminar pipe flow).

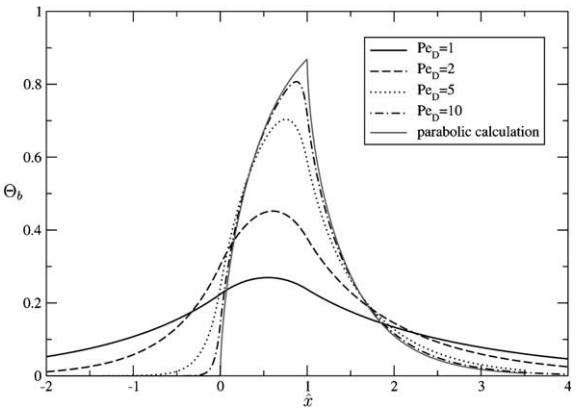

Fig. 4. Distribution of the bulk-temperature for laminar pipe flow ($\tilde{x}_1 = 0.5$) for different Peclet numbers.

scaling the x values with the length of the finite heating zone, the effect of a different length of the heating zone

can be compared easily. Fig. 5 shows the distribution of the local Nusselt number for laminar flow and different values of the Peclet number. It can be seen that the Nusselt number distribution for lower values of the Peclet number increases near the end of the heating section. This behaviour is due to the loss of heat near the end of the heating section and has also been observed in the numerical study of Hennecke [7]. In contrast to the parabolic case, the Nusselt number attains also different values after the end of the heating section, where the wall temperature has been lowered back to T_0. Fig. 6 shows the influence of a different length of the heating section on the bulk-temperature for a Peclet number of $Pe_D = 2$ for laminar flow. The figure shows clearly, how the full heating section is more and more influenced by axial heat conduction effects, if the heating section is getting shorter. This means that in such a case a parabolic calculation would be completely misleading. This can be seen even more clearly in Fig. 7, where the deviation between the Nusselt numbers from a parabolic calculation and an elliptic calculation (including axial heat conduction effects) are compared. It can be seen that the relative error $\Delta E = (Nu_{el} - Nu_{par})/Nu_{el}$ increases rapidly for the here considered Peclet number of 10, if the length of the heating section is decreased in length. For turbulent flow, the heat transfer is enhanced by the turbulent fluctuations. Fig. 8 shows a comparison of Nusselt numbers for laminar and turbulent pipe flow for a heated zone with finite length. It can be clearly seen that the general behaviour of the Nusselt number is similar, however, the absolute level of the heat transfer is of course higher for turbulent flow.

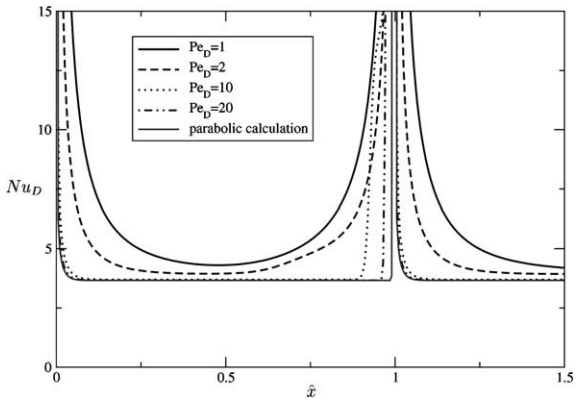

Fig. 5. Local Nusselt number for a laminar pipe flow and a finite heated section of $\tilde{x}_1 = 4$.

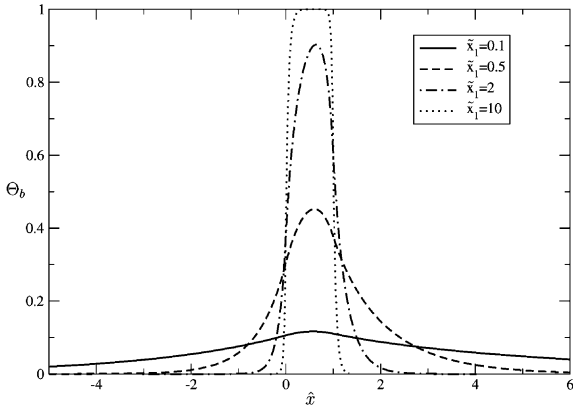

Fig. 6. Influence of the length of the heated section on the distribution of the bulk-temperature for laminar pipe flow and $Pe_D = 2$.

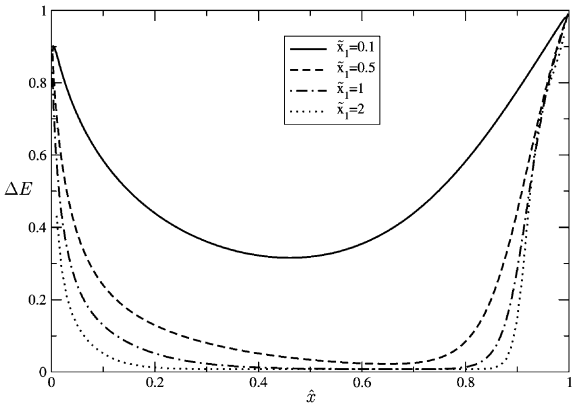

Fig. 7. Relative deviation between the local Nusselt number for a parabolic and elliptic calculation for laminar pipe flow and $Pe_D = 10$.

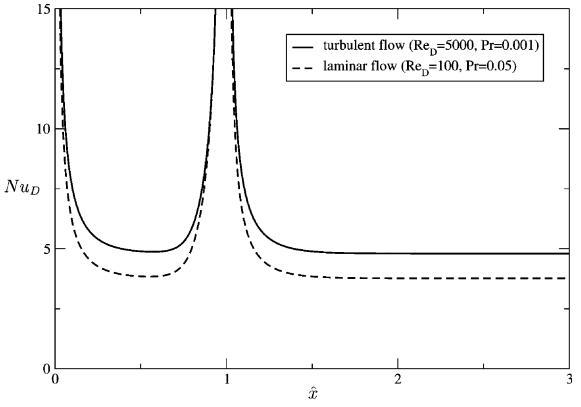

Fig. 8. Comparison of local Nusselt number distributions for laminar and turbulent flows in a circular pipe ($\tilde{x}_1 = 1$).

3.3. Heat transfer in a parallel plate channel

For flow and heat transfer in a parallel plate channel, the flow index F in the equations must be set to 0. In general one can conclude that the behaviour of the

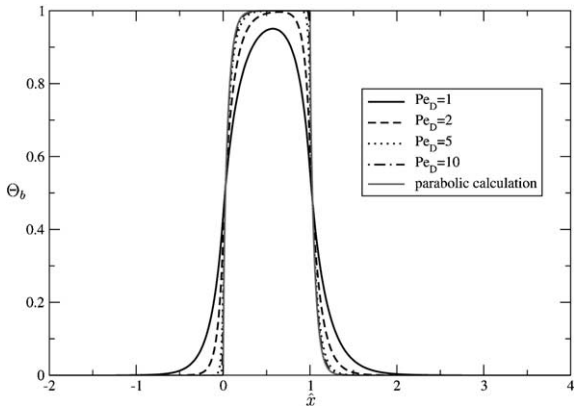

Fig. 9. Bulk-temperature for laminar flow in a parallel plate channel for different Peclet numbers.

solutions for the here considered cases is similar to the ones for a circular pipe. Fig. 9 shows the distribution of the bulk-temperature for different values of the Peclet number for a heating zone which is large ($\tilde{x}_1 = 5$). Similar to Fig. 4 it can be seen how the axial heat conduction effect lowers the values of the bulk-temperature within the heated zone. Fig. 10 shows the difference between the bulk-temperature from a simplified parabolic calculation and the present predictions for different values of the length of the heated zone. It is clearly visible, how axial heat conduction effects change the heat transfer behaviour for a short heated section. Fig. 11 compares the analytical predicted local bulk-temperature distribution with the numerical calculation by Weigand et al. [11] for a finite heated section ($Re_D = 40\,000$, $Pr = 0.01$). It can be seen that both solutions are in very good agreement.

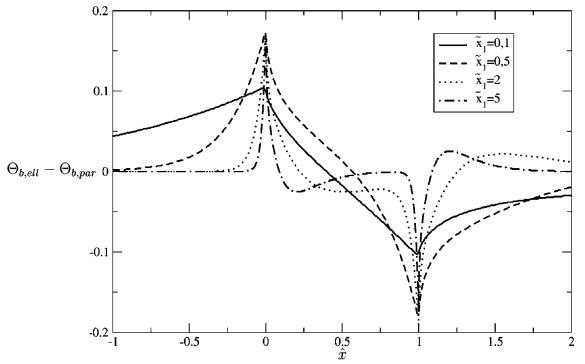

Fig. 10. Difference in bulk-temperature between parabolic and elliptic calculations for different lengths of the heating zone.

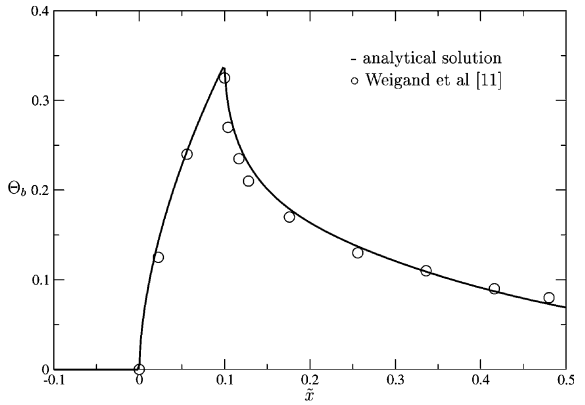

Fig. 11. Comparison between analytical and numerical solution of the bulk-temperature for a parallel plate channel with turbulent flow ($Re_D = 40\,000$, $Pr = 0.01$).

4. Conclusions

According to the present analytical study concerning the influence of axial heat conduction within the fluid, the following major conclusions can be drawn:

- Axial heat conduction effects in the fluid are important for low Peclet numbers. However, if short heating sections are considered, these effects might drastically influence the heat transfer behaviour even for higher Peclet numbers.
- The obtained analytical predictions agree well with numerical calculations from literature.
- The here presented solution is as simple and efficient to compute as the related solution of the parabolic problem.

Appendix A. In this appendix it will be shown how to obtain the following equation

$$\sum_{j=1}^{\infty} \frac{\Phi_{j2}(1)\Phi_{j1}(\tilde{n})}{\lambda_j \|\vec{\Phi}_j\|^2} = 1 \tag{A.1}$$

If one expands the vector $\vec{f} = (1,0)^{\mathrm{T}}$ into a series according to Eq. (21), one obtains for the first vector component

$$1 = \sum_{j=1}^{\infty} \frac{\Phi_{j1}}{\|\vec{\Phi}_j\|^2} \int_0^1 \frac{a_1(\tilde{n})\tilde{r}^F \Phi_{j1}}{Pe_L^2} \mathrm{d}\tilde{n} \tag{A.2}$$

Now the integral in Eq. (A.2) can be rewritten. First, one can replace the integrand by using Eq. (18). This results in

$$\int_0^1 \frac{a_1(\tilde{n})\tilde{r}^F \Phi_{j1}}{Pe_L^2} \mathrm{d}\tilde{n} = \frac{1}{\lambda_j} \left\{ \int_0^1 \tilde{u}\tilde{r}^F \Phi_{j1} \, \mathrm{d}\tilde{n} - \Phi_{j2}(1) \right\} \tag{A.3}$$

The integral on the right hand side of Eq. (A.3) can be further rewritten and one obtains

$$\frac{1}{\lambda_j}\int_0^1 \tilde{u}\tilde{r}^F \Phi_{j1}\,\mathrm{d}\tilde{n} = -\int_0^1 \frac{\Phi_{j2}}{\tilde{r}^F a_2}\left(\int_0^{\tilde{n}} \tilde{u}\tilde{r}^F\,\mathrm{d}\hat{n}\right)\mathrm{d}\tilde{n} = -\int_0^1 \Phi_{j2}\gamma(\tilde{n})\,\mathrm{d}\tilde{n} \tag{A.4}$$

Inserting Eq. (A.4) into Eq. (A.3) and this result into Eq. (A.2) gives

$$1 = -\sum_{j=1}^{\infty}\frac{\Phi_{j1}(\tilde{n})}{\|\vec{\Phi}_j\|^2}\int_0^1 \Phi_{j2}\gamma(\tilde{n})\,\mathrm{d}\tilde{n} - \sum_{j=1}^{\infty}\frac{\Phi_{j1}(\tilde{n})\Phi_{j2}(1)}{\|\vec{\Phi}_j\|^2} \tag{A.5}$$

In order to show that this expression is identical to Eq. (A.1), one has to show that the first sum on the right hand side of this equation is 0. Expanding the vector $\vec{f} = (0, \gamma(\tilde{n})\tilde{r}^F a_2)^{\mathrm{T}}$ into a series, one obtains for the first vector component

$$0 = \sum_{j=1}^{\infty}\frac{\Phi_{j1}}{\|\vec{\Phi}_j\|^2}\int_0^1 \gamma(\tilde{n})\Phi_{j2}\,\mathrm{d}\tilde{n} \tag{A.6}$$

Eq. (A.6) shows that the first sum in Eq. (A.5) is 0 and therefore, Eq. (A.1) is obtained.

References

[1] R.K. Shah, A.L. London, Laminar flow forced convection in ducts, Academic Press, New York, 1978 (Chap. V and VI).

[2] W.M. Kays, M.E. Crawford, Convective heat and mass transfer, McGraw-Hill, New York, 1993.

[3] C.B. Reed, Convective heat transfer in liquid metals, in: S. Kakac, R.K. Shah, W. Aung (Eds.), Handbook of Single-phase Convective Heat Transfer, Wiley, New York, 1987 (Chap. 8).

[4] C.J. Hsu, An exact analysis of low Peclet number thermal entry region heat transfer in transversally nonuniform velocity fields, AICHE J. 17 (1971) 732–740.

[5] E. Papoutsakis, D. Ramkrishna, H.C. Lim, The extended Graetz problem with Dirichlet wall boundary conditions, Appl. Sci. Res. 36 (1980) 13–34.

[6] C.A. Deavours, An exact solution for the temperature distribution in parallel plate Poiseuille flow, J. Heat Transfer 96 (1974) 489–495.

[7] D.K. Hennecke, Heat transfer by Hagen–Poiseuille flow in the thermal development region with axial conduction, Wärme- Stoffübertr. 1 (1968) 177–184.

[8] T.V. Nguyen, Laminar heat transfer for thermally developing flow in ducts, Int. J. Heat Mass Transfer 35 (1992) 1733–1741.

[9] S.L. Lee, Forced convection heat transfer in low Prandtl number turbulent flows: influence of axial conduction, Can. J. Chem. Eng. 60 (1982) 482–486.

[10] B. Weigand, An exact analytical solution for the extended turbulent Graetz problem with Dirichlet wall boundary conditions for pipe and channel flows, Int. J. Heat Mass Transfer 39 (1996) 1625–1637.

[11] B. Weigand, T. Schwartzkopff, T.P. Sommer, A numerical investigation of the heat transfer in a parallel plate channel with piecewise constant wall temperature boundary conditions, J. Heat Transfer 124 (2002) 626–634.

[12] B. Weigand, M. Kanzamar, H. Beer, The extended Graetz problem with piecewise constant wall heat flux for pipe and channel flows, Int. J. Heat Mass Transfer 44 (2001) 3941–3952.

[13] A.J. Reynolds, The prediction of turbulent Prandtl and Schmidt numbers, Int. J. Heat Mass Transfer 18 (1975) 1055–1069.

[14] B. Weigand, J. Ferguson, M. Crawford, An extended Kays and Crawford turbulent Prandtl number model, Int. J. Heat Mass Transfer 40 (1997) 4191–4196.

[15] A. Tamir, Y. Taitel, On the concept of the "mixing cup" temperature in flows with axial conduction, Can. J. Chem. Eng. 50 (1972) 421–424.